



HAL
open science

Physical modelling of cyclic loading on a single-helix anchor in sand

José Antonio Chiavon, Cristina de Hollanda Cavalcanti Tsuha, Luc Thorel,
Alain Neel

► **To cite this version:**

José Antonio Chiavon, Cristina de Hollanda Cavalcanti Tsuha, Luc Thorel, Alain Neel. Physical modelling of cyclic loading on a single-helix anchor in sand. EUROFUGE 2016 3rd European conference on Physical Modelling in Geotechnics, Jun 2016, NANTES, France. pp.275-279. hal-01358162

HAL Id: hal-01358162

<https://hal.science/hal-01358162v1>

Submitted on 1 Dec 2016

HAL is a multi-disciplinary open access archive for the deposit and dissemination of scientific research documents, whether they are published or not. The documents may come from teaching and research institutions in France or abroad, or from public or private research centers.

L'archive ouverte pluridisciplinaire **HAL**, est destinée au dépôt et à la diffusion de documents scientifiques de niveau recherche, publiés ou non, émanant des établissements d'enseignement et de recherche français ou étrangers, des laboratoires publics ou privés.

Physical modelling of a single-helix anchor in sand under cyclic loading

J.A. Schiavon & C.H.C. Tsuha

Department of Geotechnical Engineering, University of São Paulo, São Carlos, Brazil

A. Neel & L. Thorel

Earthworks and Centrifuge Laboratory, GERS Department, IFSTTAR, Bouguenais, France

ABSTRACT: Uniaxial tensile monotonic and cyclic loading tests have been conducted on a single-helix anchor model installed in very dense dry Hostun sand, in the IFSTTAR centrifuge. The experiments comprised different cyclic load amplitudes with maximum load up to 78% of the monotonic tensile resistance, and 2000 cycles maximum. The results contribute to clarify the effect of the number of cycles and of the load amplitude on the anchor performance.

1 INTRODUCTION

Helical anchors are frequently used in Brazil as guyed anchors for transmission line towers. In this case, the anchors are subjected to cyclic loading, from both wind and temperature variation, therefore, it is mandatory for the design to consider the effect of the cyclic loadings on the anchor behaviour.

The anchor performance under tensile cyclic loading is dependent on the cyclic load amplitude, Q_{cyclic} ; the mean load, Q_{mean} ; the period of one cycle, T ; and the number of cycles. These parameters of a cyclic loading are described in Figure 1.

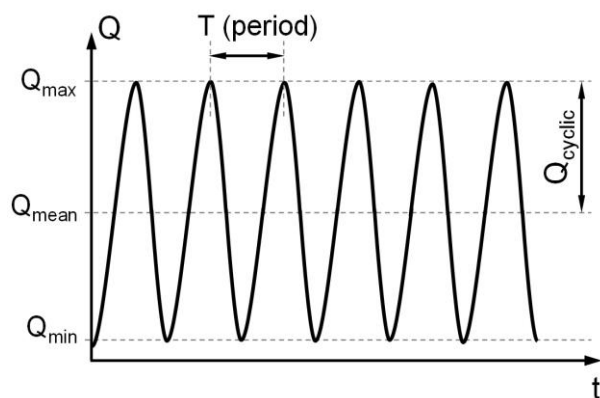


Figure 1. Cyclic loading parameters.

Two phenomena related to cyclic axial loading may influence the behaviour of helical anchors: a) the cyclic degradation of shaft friction and plate bearing resistance; b) the accumulation of permanent displacement with increasing the number of load cycles. Previous studies have reported that cyclic loading causes degradation on the anchor performance in both coarse-grain and fine-grain soils. However,

Clemence & Smithling (1984) reported that repeated loadings of low to medium amplitude improved the stiffness of the soil-anchor system. This stiffness increase can be attributed to the action of the cyclic loading on the soil above the anchor plate, which was previously disturbed by the anchor installation (Victor & Cerato 2008).

Poulos (1988) proposed a stability diagram to evaluate the response of regular piles under cyclic loading: the axis are Q_{cyclic}/Q_T versus Q_{mean}/Q_T , where Q_T is the monotonic ultimate resistance in tension. In this diagram, the pile response under different conditions of cyclic loading is classified into three zones: stable; unstable and meta-stable. Thus, it is necessary to perform several different combinations of cyclic tests to build the stability diagram of a pile in a particular soil type. To address this need, centrifuge model tests can be a valuable experimental method to investigate the behaviour of piles and anchors under cyclic loading, since parametric studies can be performed with relatively low-cost compared to full-scale tests. Therefore, this paper presents the findings of a preliminary model study on the helical anchors response to axial cyclic loading in sand. For this purpose, three cyclic tests with similar pre-load ($Q_{pre} = Q_{min}$) and different cyclic load amplitude (Q_{cyclic}) were performed in a centrifuge to simulate the wind loading on guyed towers.

2 TESTING PROGRAM

The work described here was carried out in the IFSTTAR beam centrifuge. Both model anchor installations and load tests were performed under $10\times g$ centrifuge acceleration.

2.1 Model anchor

Since the uplift capacity of a single-helix anchor is composed of shaft and helix bearing resistances, an appropriate model scale is necessary to avoid grain size effects influencing the results of the anchor response. However, no scaling laws for helical anchor models are proposed in the literature. In this case, the recommendations of previous studies about scale effects on plate model anchors and on regular model piles in sand seem to be reasonable to be applied in centrifuge modelling of helical anchors.

The prototype behaviour should be reproduced by using a minimum ratio of the rod diameter to the average soil grain-size (d/d_{50}) and of the helical plate to the average soil grain-size (D/d_{50}). In this work, the recommendations reported by Garnier *et al.* (2007) were adopted to choose appropriate shaft and helix diameters for the model anchor.

The single-helix model anchor used in the present investigation was made of steel, with a one-pitch helix of 33 mm diameter (D), with a pitch of 2.5 mm, welded to the shaft of 10 mm diameter, d (Figure 2).

Helical anchors are usually installed into the ground using a rotation rate ranging from 5 to 20 RPM, to provide a continuous and smooth advance into the soil (Chance, 2012). For the model anchor installation of this study, a rotation rate of 5.3 RPM was applied to the anchor head, simultaneously with an axial penetration rate of one helix pitch per revolution.

The model anchor was installed into the sand container with a helix embedment depth of 7.4 times the helix diameter (D), corresponding to the test system limit.

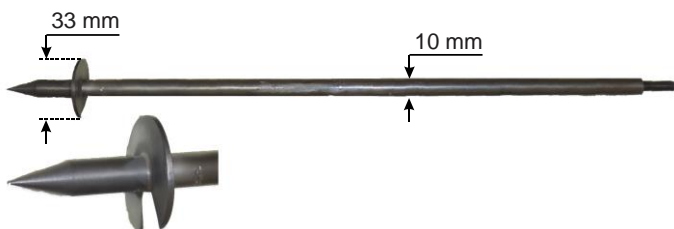


Figure 2. Helical model anchor.

2.2 Sand sample

The HN38 Hostun sand was used as soil model, with minimum dry density of 1.185 g/cm³, maximum dry density of 1.554 g/cm³, the average grain-size (d_{50}) equals to 0.12 mm and the coefficient of uniformity (C_U) equals to 1.97.

By means of the air pluviation technique, the dry sand was deposited inside a rectangular strongbox with 120 cm in length, 80 cm in width and 36 cm in depth. The sand density could be controlled by the drop height and flow rate of the sand, and by the horizontal speed of the automatic hopper. For this study,

those parameters were adjusted in order to provide a relative density (D_r) equals to 99%. Three calibrated boxes were placed at the bottom of the strongbox before the pluviation to verify the achieved dry density.

2.3 Experimental procedure

The installation of the helical anchor model was performed in flight at 10×g, for each cyclic test. After the installation, the cyclic loading was performed according to the cyclic parameters selected for each test. The parameters needed to describe the cyclic loading in tension are: (a) the mean load, Q_{mean} ; (b) the cyclic load (or the half load amplitude), Q_{cyclic} ; (c) the load frequency, f ; and (d) the number of cycles, N . The cyclic loading was applied according to a sine function with $f = 1$ Hz ($T = 1$ s) in model scale.

The cyclic pre-load (Q_{pre}) is the minimum load that the model anchor is submitted during the cyclic loading, defined as $Q_{mean} - Q_{cyclic}$. In this study, the three tests were performed with a unique tensile pre-load to simulate a pre-loaded helical anchor used for guyed towers during its service life. Table 1 presents the parameters used for the three cyclic loading tests.

Table 1. Cyclic load tests parameters

Test	Q_{pre}	Q_{mean}	Q_{cyclic}	Number of Cycles (N)
1	$0.22Q_T$	$0.32Q_T$	$0.10Q_T$	2000
2	$0.22Q_T$	$0.36Q_T$	$0.15Q_T$	2000
3	$0.22Q_T$	$0.50Q_T$	$0.28Q_T$	1000

The test procedure, from the sample preparation to the cyclic testing in flight, is described below:

- a) The sand sample is reconstituted by air pluviation.
- b) The sand sample is embarked in the centrifuge swinging basket.
- c) The servo-controlling system is installed over the strongbox (Figure 3).
- d) Three consecutive stabilization cycles of centrifugation, with three minutes duration and 10×g centrifuge acceleration are performed.
- e) The model anchor is installed in flight.
- f) Three minutes of waiting after model installation.
- g) The pre-tensile load is applied.
- h) Three minutes of waiting after applying pre-tensile load.
- i) The cyclic loading is performed.
- j) The anchor pull-out test is carried out with a loading rate of 0.3 mm/s.
- k) The centrifuge is stopped for repositioning the servo-controlling system to the next anchor test.
- l) items e) to k) are repeated for the following test.

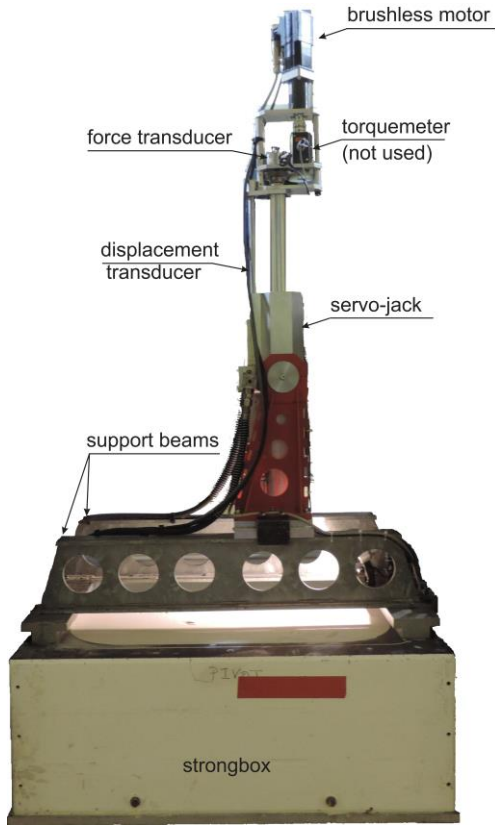


Figure 3. Strongbox and servo-controlling system.

3 RESULTS

Three cyclic tests have been performed on three different anchor tests (one cyclic test per anchor). Before the cyclic loading test campaign, a monotonic pull-out test was carried out to determine the monotonic uplift capacity and to define the cyclic load amplitude for each test. In addition, a second pull-out test was conducted on the same model anchor following the first monotonic test intending to compare the load-displacement responses from both monotonic tests.

3.1 Monotonic pull-out tests

The load-displacement response of the monotonic pull-out is presented in Figure 4. Two different trends can be observed in the portion before the peak load in this figure: a linear zone from zero to around $0.03D$ of vertical displacement, followed by a non-linear behaviour until a vertical displacement around $0.2D$. An ultimate load (Q_T) of 93 kN in prototype scale (assumed as the maximum load registered in the load test) was attained after 54.6 mm ($0.16D$) of anchor head displacement, in prototype scale. At $0.1D$ of vertical displacement, the measured tensile load was 89 kN (prototype scale), a relative small difference comparing to the ultimate peak value.

After 400 mm of vertical displacement in prototype scale, the model anchor was unloaded and showed 6.7 mm of recoverable displacement. Then, a second tensile load test was performed to investi-

gate the monotonic behaviour after large displacements. Figure 5 compares the load-displacement responses of both pull-out tests. The initial portion of both curves is similar until around 50% of the ultimate load of the first test (Q_T), equivalent to the service load condition for a safety factor of 2. Unlike in the first test, the non-linear second portion of the curve preceding the peak load was not observed in the second test. The effect of a prior tension loading with large displacements reduced the anchor pull-out capacity to 65% of the initial value. In this case, the anchor failure occurred at a vertical displacement of $0.04D$.

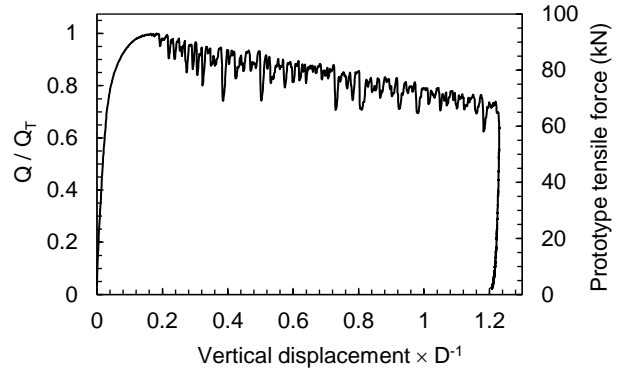


Figure 4. Monotonic load-displacement response.

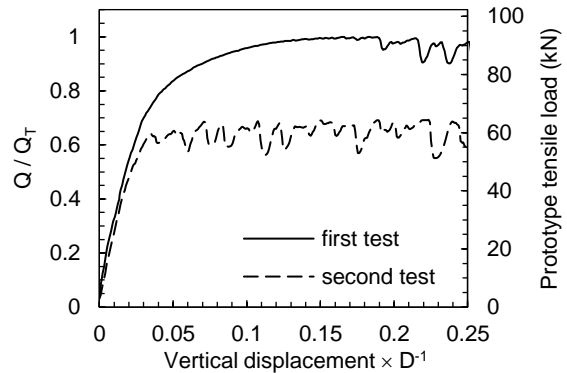


Figure 5. Anchor response to consecutive tests.

The soil disturbance under the helix due to unloading and pull-out was not evaluated in this work. Mosquera *et al.* (2015) present photographs of the dry sand mass around a single-helix anchor model with 40 mm helix diameter after the installation and after the tension load test. Mosquera *et al.* observed that the sand mass under the helix was pressed down after the anchor installation. After an uplift displacement of $0.2D$ (8 mm in model scale), a gap below the helix was observed with no occurrence of sand movement toward this gap. In this case, the load-displacement response is controlled by the properties of disturbed soil above the helix. Thus, negligible influence of the soil properties below the helix is assumed for the case of one-way tensile load.

3.2 Cyclic loading

The maximum downward force applied to the model anchor head during the installation varied between 63 kN and 70 kN (in compression), in prototype scale. The vertical displacements were monitored from the end of each model installation to the beginning of the cyclic loading (item f to h described in section 2.3). This displacement trajectory comprises a portion induced by the relief of the compression load applied to the model head during the installation. A second portion of the displacement trajectory is due to the application of the pre-tensile load. To apply the pre-tensile load after the end installation, the vertical displacements of the anchor model head in prototype scale was 5.4 mm in Test 1, 5.0 mm in Test 2 and 4.8 mm in Test 3.

The cyclic loading of each test was performed after the anchor installation. No prior loading was applied to the model anchor before the cyclic test (except the pre-tensile load). Three different amplitudes of cyclic loading were investigated, using the same pre-load value (Q_{pre}).

Due to a configuration error in programming the servo-controlling system, the cyclic loading started in advance, resulting in a slope of the applied load in the firsts 12 and 50 cycles of the Test 2 and Test 3, respectively.

Figure 6 presents the three different load-displacement response of the anchor under cyclic loading. The displacements observed in the first cycle are larger and differ significantly from the following cycles. The difference in the first cycle occurs because this cycle corresponds to the very first loading on the disturbed sand above the helix. This result indicates that the anchor initial stiffness is reduced due to the sand disturbance above the helical plate caused by the anchor installation.

Amongst the three tests, only Test 3 reached anchor displacements greater than $0.1D$ (33 mm in prototype scale). The accumulated vertical displacement after 1000 cycles was 6.8 mm ($0.02D$) in Test 1, 14.7 mm ($0.04D$) in Test 2, and 35.3 mm ($0.11D$) in Test 3 in prototype scale. For Tests 1 and 2, the cyclic loading was carried out until 2000 load cycles, and the accumulated vertical displacements at the end of the cyclic tests were 8.7 mm and 18.0 mm in prototype scale, respectively.

In Figure 7, two different displacement accumulation responses are identified. The three tests exhibited a bi-linear relationship of the vertical displacement to the logarithm of the number of cycles. However, the intersection point of the bi-linear curve was not the same for all tests. The sharp change occurred after few cycles for tests with greater cyclic load amplitudes. In Test 1, for example, the displacements accumulation changes after 400 cycles, approximately. In Test 2, this transition is observed around 100 cycles, and around 20 cycles in Test 3.

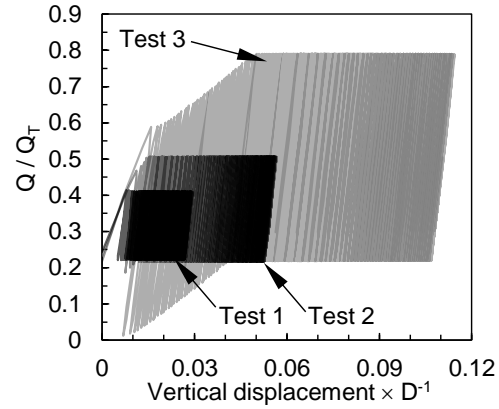


Figure 6. Cyclic tests load-displacement responses.

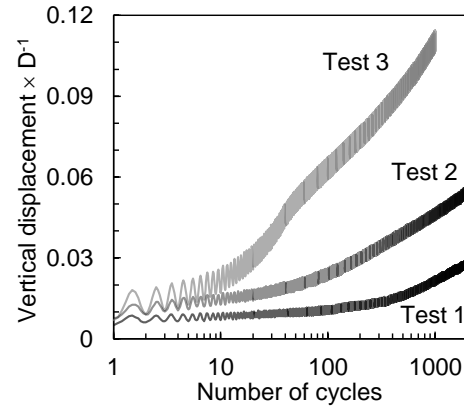


Figure 7. Normalized vertical displacements vs number of cycles.

In this study, an unstable cyclic response was identified when the accumulated anchor head displacement increase rapidly, leading to accumulated displacements equal or greater than $0.1D$ with less than 100 cycles (Tsuha *et al.*, 2012). Therefore, none of the three tests exhibited unstable response.

The stable cyclic response was recognized for cases in which the head displacement accumulates slowly, and do not achieve the $0.1D$ value after 1000 cycles. The cyclic loadings did not cause accumulated displacements greater than $0.1D$ after 1000 cycles and after 2000 cycles for Tests 1 and 2. Therefore, cyclic loadings with $Q_{max} = 0.5Q_T$ or less did not lead to the failure caused by cumulative displacements.

On the other hand, the cyclic loading of the Test 3, with $Q_{max} = 0.8Q_T$, showed accumulated displacements greater than $0.1D$ after 480 cycles, corresponding to a meta-stable response (cumulative displacements attain $0.1D$ among 100 and 1000 cycles). Despite this, in this same Test 3, the anchor head displacements exhibited no significant growth after 1000 cycles, reaching a cumulative displacement of 11% of the helix diameter after 2000 cycles.

For all the tests, the rate of displacement accumulation was more significant over the first 100 cycles. This accumulation occurs because the soil above the helical plate is disturbed due to the installation process, and the anchor stiffness may increase due to the soil densification above the plate caused by the cy-

clic loading. The stiffness increase contributes to the anchor cyclic stability, and prevents the cyclic failure of the model anchor under cyclic loading with large values of Q_{max} .

4 CONCLUSIONS

Three different cyclic load tests on a single-helix anchor in dry sand were performed using a geotechnical centrifuge. The results of this investigation have indicated a bi-linear relationship of the anchor displacement to the logarithm of the number of cycles. In addition, the tested single-helix anchor has shown cyclic stable response for cyclic amplitudes ($2Q_{cyclic}$) up to 30% of the ultimate tensile load (Q_T), with a pre-load Q_{pre} around $0.2Q_T$.

ACKNOWLEDGMENTS

The authors would like to acknowledge the financial support provided by the Brazilian Agency CAPES and by the IFSTTAR. We also would like to thank the assistance provided by P. Gaudicheau, P. Au drain, S. Lerat, D. Macé and C. Favraud.

REFERENCES

- Chance Civil Construction. 2012. *Guide to model specification: helical piles for structural support*. Bulletin 01-0303, Centralia.
- Clemence, S.P. & Smithling, A.P. 1984. Dynamic uplift capacity of helical anchors in sand. *Proc. 4th Australia-New Zealand conf. geomech, 1984*.
- Garnier, J. et al. 2007. Catalogue of scaling laws and similitude questions in geotechnical centrifuge modelling. *Int. J. Phys. Mod. Geotech.* 7(3): 1-23.
- Mosquera, Z.S.Z. et al. 2015. Discussion of "Field investigation of the axial resistance of helical piles in dense sand". *Can. Geotech. J.* 52(8): 1190-1194.
- Poulos, H.G. 1988. Cyclic stability diagram for axially loaded piles. *Geotech. Engrg. Div. ASCE* 114(8): 877-895.
- Tsuha, C.H.C. et al. 2012. Behaviour of displacement piles in sand under cyclic axial loading. *Soils and found.* 52(3): 393-410.
- Victor, R.T. & Cerato, A.B. 2008. Helical anchors as wind tower guyed cable foundations. *Proc. 2nd BGA int. Conf. on found. (ICOF2008), Dundee, 2008*.